

# Transient cavity studies

Stephen Molloy

April 13, 2012

## 1 Introduction

The response of superconducting cavities to being driven by an external RF source may be described by a first-order differential equation. Solutions to this may be obtained computationally by discretising the equation, and an analysis of the output can indicate, among other things, the total energy reflected from each cavity during a single machine cycle.

This note presents the equations governing this process, their discretisation, and some initial studies of the reflected energy, etc. The necessary initial conditions are also discussed, and the expected reflected energy from the entire superconducting linac is shown.

## 2 LCR circuit equation

The voltage,  $V(t)$ , and current,  $I(t)$ , observed in the LCR circuit analogy of a superconducting accelerating cavity may be split into their real and imaginary components with the fast RF oscillation separated out as follows,

$$V(t) = (V_r(t) + iV_i(t)) \cdot e^{i\omega t} \quad (1)$$

$$I(t) = (I_r(t) + iI_i(t)) \cdot e^{i\omega t} \quad (2)$$

Where the subscripts,  $r$  and  $i$ , refer to the real and imaginary components respectively, and the RF has a frequency,  $f = \omega/2\pi$ .

These may be inserted into the differential equation describing the time evolution of a driven LCR circuit, resulting in the following

$$\frac{dx(t)}{dt} = A \cdot x(t) + B \cdot u(t) \quad (3)$$

Where,

$$A = \begin{pmatrix} -\omega_{1/2} & -\Delta\omega \\ \Delta\omega & -\omega_{1/2} \end{pmatrix} \quad (4)$$

$$B = \begin{pmatrix} R_L\omega_{1/2} & 0 \\ 0 & R_L\omega_{1/2} \end{pmatrix} \quad (5)$$

$$x = \begin{pmatrix} V_r \\ V_i \end{pmatrix} \quad (6)$$

$$u = \begin{pmatrix} I_r \\ I_i \end{pmatrix} \quad (7)$$

Where the cavity bandwidth,  $\omega_{1/2} = \omega_0/2Q_L$ , the detuning of the cavity,  $\Delta\omega = \omega_0 - \omega$ , and the coupler-loaded resistance of the cavity equivalent circuit,  $R_L = (R/Q) Q_L$ .

Equation 3 thus describes the evolution of the accelerating field present in a general cavity. The driving term,  $u$ , is the vector sum of the current excited by the generator,  $I_g$ , (e.g. a klystron) and that excited by the beam,  $I_{beam}$ .

### 3 Numerical solutions

Equation 3 may be solved for a general driving term,  $u$ , using standard numerical techniques. It is first converted into a discrete form that can be implemented in computer code.

$$\frac{x_2 - x_1}{\Delta t} = A \cdot x_1 + B \cdot u_1 \quad (8)$$

Here the subscripted parameters,  $x_1$ ,  $u_1$ ,  $x_2$ , and  $u_2$ , refer to the value of those parameters at different times,  $t_1$  |  $t_2$ , etc. The difference between those times,  $\Delta t = t_2 - t_1$ , should be small with respect to the characteristic time-scale of the cavity,  $\tau = 2Q_L/\omega_0$ , where the loaded quality factor,  $Q_L$ , and cavity frequency,  $f = \omega/2\pi$ , are used.

From equation 8, it is trivial to rearrange to solve for  $x_2$ .

$$x_2 = \Delta t (A \cdot x_1 + B \cdot u_1) + x_1 \quad (9)$$

Given an initial condition for the voltage,  $x(t = 0)$ , and a driving current,  $u(t)$ , equation 9 can then be used to derive each subsequent value for the voltage,  $x(t)$ , for every value of  $t$  for which the driving current is defined.

## 4 Studies

The algorithm shown in equation 9 has been implemented as a set of Python classes & methods, and used to derive the following results.

The value of the time step used in all studies presented here is  $\Delta t = 10^{-3}\tau$ .

### 4.1 Well optimised cavity

Parameter	Value
RF frequency	704.42 MHz
Accelerating voltage	18 MV
R/Q	477 $\Omega$
$Q_L$	$7.778 \times 10^5$
Design beam current	50 mA
Operating beam current	50 mA
Synchronous phase	-14.0 $^\circ$
Geometric $\beta$	0.90
Beam $\beta$	0.90

Equation 9 was used to determine the voltages excited in a perfectly optimised cavity. The beam and cavity parameters used for this calculation are shown in table 4.1. Note that the value of the loaded Q,  $Q_L$ , was calculated to

be optimal for the other parameters. The detuning of the cavity is not shown in this table, but was set to cancel the synchronous phase of the beam.

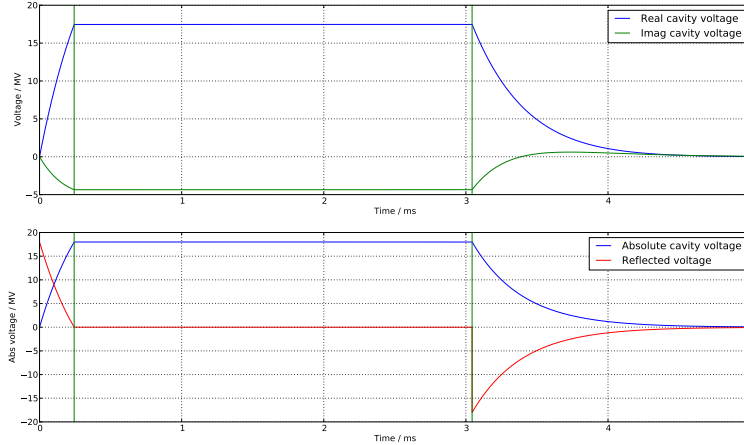


Figure 1: Time evolution of the cavity voltage when drive by the correct current.

Figure 1 shows the calculated real & imaginary cavity voltage, as well as the absolute voltage excited in the cavity, and the field reflected back from the coupler.

Note the detuning of the cavity means that the cavity voltage has a non-zero imaginary component values showing that the cavity voltage has a non-zero phase with respect to the beam<sup>1</sup>.

Observe how the beam injection time, indicated by the first horizontal line, is set so that the cavity voltage has climbed to the correct value at this time. Also notice that after this time, the gradients of the cavity voltage and beam excited signals are equal and opposite, thus causing the voltage to remain constant during the passage of the beam.

Once the beam pulse has ended, the RF drive is switched off, and the cavity fields decay exponentially to zero with a time constant related to the  $Q_L$  of the cavity.

Figure 2 shows the driving currents used for this calculation, as well as the reflection coefficient.

It can be seen that the amplitude of the klystron drive remains constant until the end of the beam pulse, but that there is a phase change when the beam arrives. The phase of the driving current before the arrival of the beam is calculated so that the voltage excited in the cavity has reached the correct value when the beam is injected. After this point however, the cavity is being driven by a combination of the klystron and beam currents, and so will tend towards a different steady-state phase. Therefore the phase of the klystron drive must be changed in order that this steady-state value is equal to that specified by the lattice designers.

<sup>1</sup>The reference phase is defined such that the beam excited signal lies purely along the negative real axis.

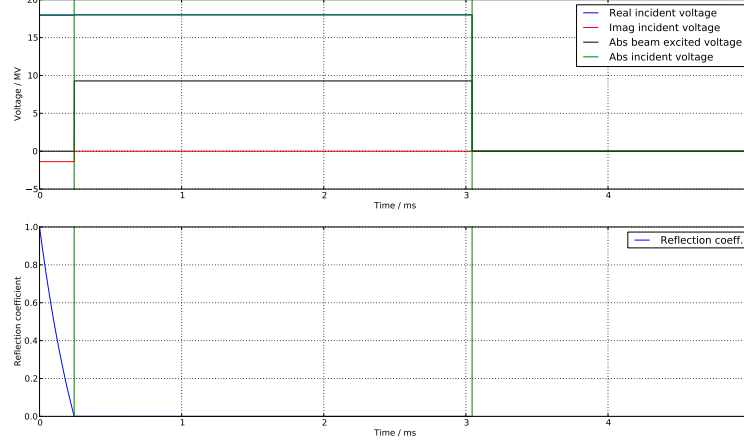


Figure 2: Klystron and beam related driving currents responsible for the voltages in figure 1, as well as the reflection coefficient defined as the ratio between the reflected and incident voltages.

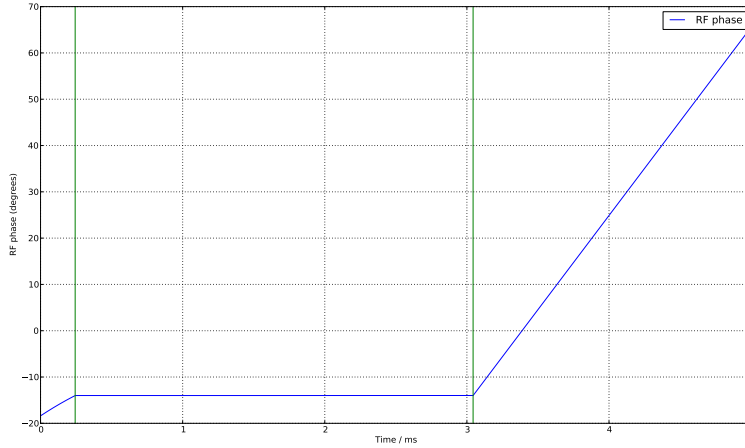


Figure 3: Phase of the cavity voltage.

In order to determine the phase of the driving term before beam-arrival, it is necessary to calculate how the phase of the cavity voltage will evolve with time. It can be shown that the real and imaginary components of the voltage evolve as follows.

$$V_r(t) \propto e^{-\omega_{1/2}t} (-\omega_{1/2} \cos(\Delta\omega t) + \Delta\omega \sin(\Delta\omega t)) + \omega_{1/2} \quad (10)$$

$$V_i(t) \propto e^{-\omega_{1/2}t} (-\omega_{1/2} \sin(\Delta\omega t) - \Delta\omega \cos(\Delta\omega t)) + \Delta\omega \quad (11)$$

The expected phase change between  $t = 0$ , and the time of beam injection,  $t = t_{inj}$ , can then be found as follows.

$$\phi(t=t_{inj}) = \arctan\left(\frac{V_i(t_{inj})}{V_r(t_{inj})}\right) \quad (12)$$

Since the phase of the drive during the beam pulse is set so as to result in the correct synchronous phase,  $\phi_b$ , being achieved, the pre-beam driving current should be calculated by rotating the beam pulse drive by the difference between  $\phi_b$  and the phase change calculated from equation 12.

The result of this manipulation on the phase of the cavity voltage phase is shown in figure 3, and it can be seen that the desired result has been achieved.

The power reflected from the cavity,  $P_{ref}$ , can be calculated from the reflected voltage,  $V_{ref}$ .

$$P_{ref} = \frac{V_{ref}^2}{\left(\frac{R}{Q}\right) Q_L} \quad (13)$$

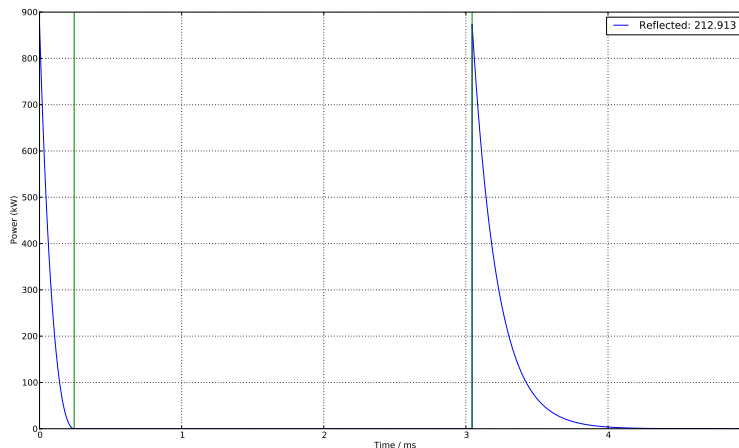


Figure 4: Power reflected from the optimised cavity, along with a calculation of the total energy reflected back to the load.

The power reflected from the optimised cavity is shown in figure 4, as well as a calculation of the total energy reflected in this pulse.

This represents a best case scenario. Even when the machine is running with the nominal parameters, many of the cavities will be operating significantly far from their optimal performance due to the spread of accelerating voltages, beam velocities, etc., required by beam dynamics considerations.

## 4.2 Nominal linac

Figure 5 shows the magnitude of the energy reflected per pulse for each cavity in the linac, and it can be seen that the RF distribution system should be capable of handling up to  $\sim 225$  J of reflected energy per pulse, even during nominal, fault-free, machine operation.

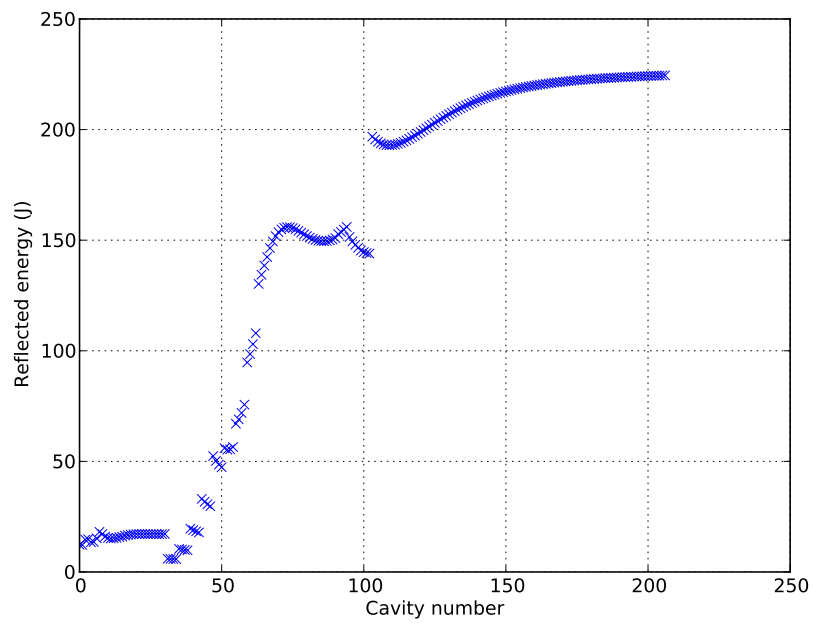


Figure 5: Energy reflected from each cavity in the linac.